



Preparation and Characterization of Iron Oxide Nanoparticles for Effective Epirubicin Delivery to Drug Resistant Breast Cancer Cells

Sayra Tariq, Zeeshan Mutahir and Moazzam Ali*

School of Biochemistry and Biotechnology, Quaid e Azam Campus, University of the Punjab, Lahore, Pakistan.

ABSTRACT

Chemoresistance is toughest of all challenges in the fight against cancer. The incorporated drugs are pumped out of the cells due to a number of reasons. However, if these drugs are attached to nanoparticles, they are likely to be retained by the cells for longer period of time. In this study, iron oxide nanoparticles were synthesized using green synthesis and studied for their drug release and anticancer properties. Scanning electron microscope (SEM) analysis results showed that the average size of the synthesized spherical iron oxide nanoparticles was around 48nm, which was further confirmed with transmission electron microscopy (TEM) images. Anticancer drug, epirubicin was attached to the iron oxide nanoparticles. Immobilization of epirubicin on the nanoparticles was confirmed by FTIR analysis (Fourier-transform infrared spectroscopy). The spherical nanoparticles showed rapid pH sensitive drug release at pH 4.9 (pH of the cancer cell) targeting the tumor microenvironment and the cancer cell or endosomes/lysosomes. Drug loaded nanoparticles showed increased zones of inhibition as compared to naked iron oxide nanoparticles. After adsorbing on the nanoparticle surface, the loaded drug exhibited potent cytotoxic effect on drug sensitive (wt) and epirubicin resistant (epi-R) breast cancer cell lines MDA-MB-231 in a dose dependent manner. MDA-MB-231/ epi R cells showed viability of 71.59% against 20 μ M epirubicin, however it decreased to 58.19% when the cells were exposed same concentration of epirubicin loaded on Iron oxide nanoparticles. The pattern of increased efficacy of drug loaded nanoparticles was observed in wound healing assay carried out with both MDA-MB-231/wt and epirubicin resistant cells. Percentage healing after 24 h with 10 μ M epirubicin alone was 38.1% for MDA-MB-231/epi-R cells. This further decreased to 32.35% when cells were exposed to 10 μ M epirubicin loaded on iron oxide nanoparticles. This study shows the ability of iron oxide nanoparticle-based drug delivery system for carrying the drug, and effectively releasing it for drug sensitive as well as drug resistant breast cancer cells.

Article Information

Received 27 February 2023

Revised 28 September 2023

Accepted 10 October 2023

Available online 29 December 2023
(early access)

Authors' Contribution

ST performed the experimental work and wrote the manuscript. ZM helped in data analysis and manuscript preparation. MA conceived the study, helped in data analysis and edited the manuscript.

Key words

Chemo-resistance, iron oxide nanoparticles, epirubicin, breast cancer, MDA-MB-231

INTRODUCTION

Failure of chemotherapy in cancer patients involves the overexpression of certain proteins that pump the drug out of the cell (Zulberg *et al.*, 2016). This situation is further aggravated when the chemotherapeutic agent starts attacking the normal healthy cells along with the tumor cells. Therefore, it is very important to come up with modern strategies to selectively target chemotherapeutic agent to tumor site (Saeed *et al.*, 2018).

Nanotechnology however has been an area of specific

interest when strategies involving overcoming chemo resistance, and targeted drug delivery are discussed (Cheng *et al.*, 2013). The main advantage lies in the small size of the particles that ensure a safe delivery of chemotherapeutic agent and nucleotide therapeutics to the target site (Dunkan, 2003). Other advantages include ensuring accumulation of drugs in the tumor, protecting the normal tissues by enhancing the immunity of the body and focusing on improving the bioavailability of drugs that have poor physiochemical characteristics (Liang *et al.*, 2010). Nanoparticle based drug delivery systems are used now a days to facilitate targeted delivery of drug to the target tumor site (Farokhzad and Langer, 2009). One of the widely used particles specifically for cancer treatment are iron oxide nanoparticles (Sidhwani *et al.*, 2020). Iron oxide nanoparticles are in focus because they exhibit super paramagnetic behavior, are low in cost, easily biodegradable and have a good biocompatibility. The particles are either allowed to reach the target site through blood circulation or, are monitored with the help of an external magnetic field (Ruenraroengsak *et al.*, 2010). The drug release at

* Corresponding author: moazzam.ibb@pu.edu.pk
0030-9923/2023/0001-0001 \$ 9.00/0



Copyright 2023 by the authors. Licensee Zoological Society of Pakistan.

This article is an open access article distributed under the terms and conditions of the Creative Commons Attribution (CC BY) license (<https://creativecommons.org/licenses/by/4.0/>).

the target site can be due to one or more of physiological changes like changes in osmolality, temperature, pH or can be due to enzymatic activity inside the tumor (Muthu *et al.*, 2009; Regu *et al.*, 2020). It has been studied that epirubicin, a chemotherapeutic drug, binds to the surface of nanoparticles through a covalent bond that is pH sensitive (Unsoy *et al.*, 2014). This pH sensitive bond breaks under acidic conditions that is excellent for a tumor microenvironment that usually exhibits pH range between 4.8 to 5.2 (Yue *et al.*, 2014). Iron oxide nanoparticles exhibit controlled release of drug at the tumor site. These particles are commercially available and are currently being used as MRI contrast enhancement agents (Ali *et al.*, 2016).

The synthesis of nanoparticles can either be chemical method or green synthesis using various plants extracts (Oskum, 2006; Awwad and Salem, 2012). The use of chemicals for synthesis of nanoparticles has adverse effects on both, the environment and the organism (Arami *et al.*, 2015). Also, chemical synthesis has high production costs and releases harmful chemicals to the environment. Green synthesis avoids the production of harmful byproducts using eco-friendly synthesis procedures (Jagwani and Hari, 2021; Yew *et al.*, 2020). Availability of phytochemicals in various plants extracts helps in synthesis of these particles (Ameen *et al.*, 2020). Also, the solvent required for the synthesis is pure distilled water which is readily and easily available (Saif *et al.*, 2016). Green tea has always been a center of attention not only for its role in health and disease but also as a reducing agent for nanoparticle synthesis (Afzal *et al.*, 2015). It produces small sized particles and has no potential hazardous side chemicals (Weng *et al.*, 2017).

The purpose of this study was to synthesize biocompatible iron oxide nanoparticles through green synthesis and evaluating their efficiency as a drug carrier. Epirubicin is linked to the particle through a pH sensitive bond that is quite stable at normal physiological pH 7.4 and is easily degraded under acidic conditions of the tumor. The in-vitro anticancer activity of epirubicin was determined in MDA-MB-231 breast cancer cell lines both drug sensitive (wild type) and 500 nM epirubicin resistant (epi-R). Results were further confirmed using scratch healing assay. Antimicrobial activity was also assessed against different pathogenic strains of bacteria.

MATERIALS AND METHODS

Materials

The main chemical used in green synthesis of iron oxide nanoparticles was anhydrous FeCl₃ 97% from icon chemical. Lipton green tea was purchased from a local vendor. Epirubicin hydrochloride (trade name Farmorubicin CS 50mg/25 ml from Pfizer) was used for

drug loading. Breast cancer cell line MDA-MB-231 was obtained from School of Biochemistry and Biotechnology, University of the Punjab Cell Culture Lab. The cells were cultured in high glucose DMEM medium with 10% fetal bovine serum, both from Thermo Fisher Scientific. 100 units/mL penicillin-streptomycin (obtained from Thermo Fisher Scientific), was added to the media. Deionized water was used for solution preparations.

Preparation of green tea extract

Sixty grams of dry green tea was added to 1000 ml deionized water and the solution was heated to 80 °C in a water bath. The extract was first strained to remove all green tea leaves followed by filtration through Whatman filter paper number 2. The filtrate was placed in a clean container and stored at 4 °C for further use.

Iron oxide nanoparticle synthesis

Iron oxide solution was added to the green tea extract in a 2:1 ratio. Green tea extract was placed on a magnetic stirrer and was heated to 50 °C with continuous stirring at 400 rpm. 0.1M Ferric chloride solution was added drop wise to the extract. The green tea extract showed an abrupt change in color after the addition of ferric chloride solution. The mixture was kept on stirring at 50 °C for 30 min. The mixture was centrifuged at 10,000 g for 20 min. The supernatant was discarded. The pellet was washed twice with water and twice with ethanol with centrifugation at 10,000 g for 20 min each time. Ethanol was used to remove all kinds of impurities in green synthesized nanoparticles that were left after washing with water. The pellet was lyophilized to get stable dry iron oxide nanoparticles. The particles were stored in an Eppendorf tube in a dry place for further use.

Preparation of drug loaded iron oxide nanoparticles

Lyophilized nanoparticles (200mg) were sonicated with a probe sonicator for 2 min in 10 ml of absolute ethanol to disperse the particles for an efficient uptake of drug. The mixture was centrifuged at 200g for 2 min to separate larger particles. The supernatant was further centrifuged at 14000 g for 10 min. Ethanol in the supernatant was discarded and particles were allowed to dry up in a biosafety cabinet. Epirubicin in the concentration 0.2 mg/ml was added to the particles, making the final volume up to 1ml with PBS. The mixture of nanoparticles and drug was kept in a rotary shaker at 37 °C. The drug uptake was calculated by measuring the spectrophotometric absorption of supernatant at 498 nm, comparing it with the absorption at the start of uptake. After drug uptake, the nano particles were centrifuged at 14,000 g for 10 min and were washed twice with sterile distilled water. The sterile drug loaded

particles were resuspended in PBS and stored at 4 °C.

Physiochemical characterization of nanoparticles

Synthesized iron oxide nanoparticles were characterized through X-Ray diffraction (XRD) analysis, scanning electron microscope (SEM), energy-dispersive X-ray (EDX) and Fourier-transform infrared (FTIR) analysis. Phase purity and crystallinity of nanoparticles was investigated by XRD (model PANalytical Xpert Pro DY3805 Powder XRD). FTIR was carried out using Model Nicolet 6700 with mode of transmission – atr, wavelength range 4000-650 for atr 4000-400 transmission for films, gas was nitrogen and the number of scans were 128 at resolution 8. Structural properties were observed by SEM analysis using SEM machine model JEOL JEM2010 from Japan. TEM analysis was made using TEM (2010F-UHR-JEOL-Tokyo, Japan).

Assessment of antimicrobial activity of nanoparticles

Nanoparticle's antimicrobial activity was assessed through the agar well method. Nutrient agar media was prepared and autoclaved. Sterilized media were poured and set aside to solidify in sterile petri plates. Overnight cultures of *E. coli* and *S. aureus* in nutrient broth having 10^5 CFU/ml were inoculated on agar media plates. 50 μ g/100 μ L nanoparticles poured into the wells and were incubated at 37 °C for 24 h. Zones of inhibitions (ZOI) were measured in millimeters for both plates.

Maintenance of human cancer cell lines

Human breast cancer cells, MDA-MB-231; drug sensitive (wild type) and 500 nM epirubicin resistant (epi-R) were maintained following standard procedures. Briefly, cells were cultured in DMEM high glucose medium supplemented with 10% FBS and penicillin/streptomycin in vented cell culture flasks and were kept in a CO₂ incubator at 37 °C with 5% CO₂. Cells were passaged by trypsinization as and when required using 0.05% trypsin after washing with Ca⁺⁺, Mg⁺⁺ free DPBS. The drug resistant variant was kept under constant pressure of 500 nM epirubicin.

Cytotoxicity of epirubicin loaded nanoparticles

MTT cytotoxicity assay was performed to assess the cytotoxic potential of epirubicin loaded nanoparticles. Cells were seeded at 8000 cells per well in a 96 well cell culture plate and were incubated in a CO₂ incubator at 37 °C for 24 h. Varying concentrations of epirubicin along with equivalent concentration of epirubicin loaded nanoparticles and drug free nanoparticles were added to cells by serial dilution. The plate was incubated for 72h.

Cytotoxicity assay was performed by adding 10 μ l of 5mg/ml MTT to each well and the cells were incubated for another four h. All liquid content was then removed from the wells and 100 micro liters of acidified isopropanol was added to solubilize the formazan crystals. Plate was read at 492nm and percentage viability was calculated by normalizing drug containing wells to no drug controls.

Wound healing assay

0.2 million cells were seeded in a six well cell culture plate with 2 ml media in each well. Cells were allowed to grow in a CO₂ incubator under standard conditions. Once the cells got confluent a scratch was made in the middle of the well with the help of 200 μ l pipette tip angled at 45°. Cells were washed once and were replenished with reduced serum medium and varying concentrations of epirubicin and nanoparticles. Cells were observed at 0, 6, 12 and 24 h under an inverted phase contrast microscope at magnification of 4X.

RESULTS

SEM analysis

Iron oxide nanoparticles were synthesized using green tea leaves as reducing agents. The particles were black in color when synthesized. Surface morphology and size of the prepared nanoparticles was analyzed by SEM micrographs. Figure 1A shows the spherical morphology of iron oxide nanoparticles (NPs). Most of the iron oxide NPs were spherical in structure however cubic shaped NPs were also observed. The images showed excessive agglomeration because of the particles remaining in solution for long. The average size of the particles was between 40-50nm. In order to further confirm the morphology and size distribution of the prepared iron oxide nanoparticles, the particles were subjected to TEM analysis which confirmed the size obtained by the SEM analysis (Fig. 1B).

XRD and FTIR analyses

X-ray power diffraction was used to confirm the phase purity and crystallinity of green synthesized iron oxide nanoparticles. Figure 2A represents of XRD pattern of IO NPs. The XRD diffraction pattern unveil characteristic sharp peaks of IO NP indexed at 2 theta = 30.2, 35.5, 43.0, 57.3 and 62.9 attributed to 220, 311, 400, 511 and 440 crystallographic planes which matched exactly with JCPDS file no: 65-3107. The sharp peaks observed in the graph are a clear indication of high crystallinity of synthesized green nanoparticles. Nonappearance of additional peaks confirmed the absence of any impurities in the synthesized particles.

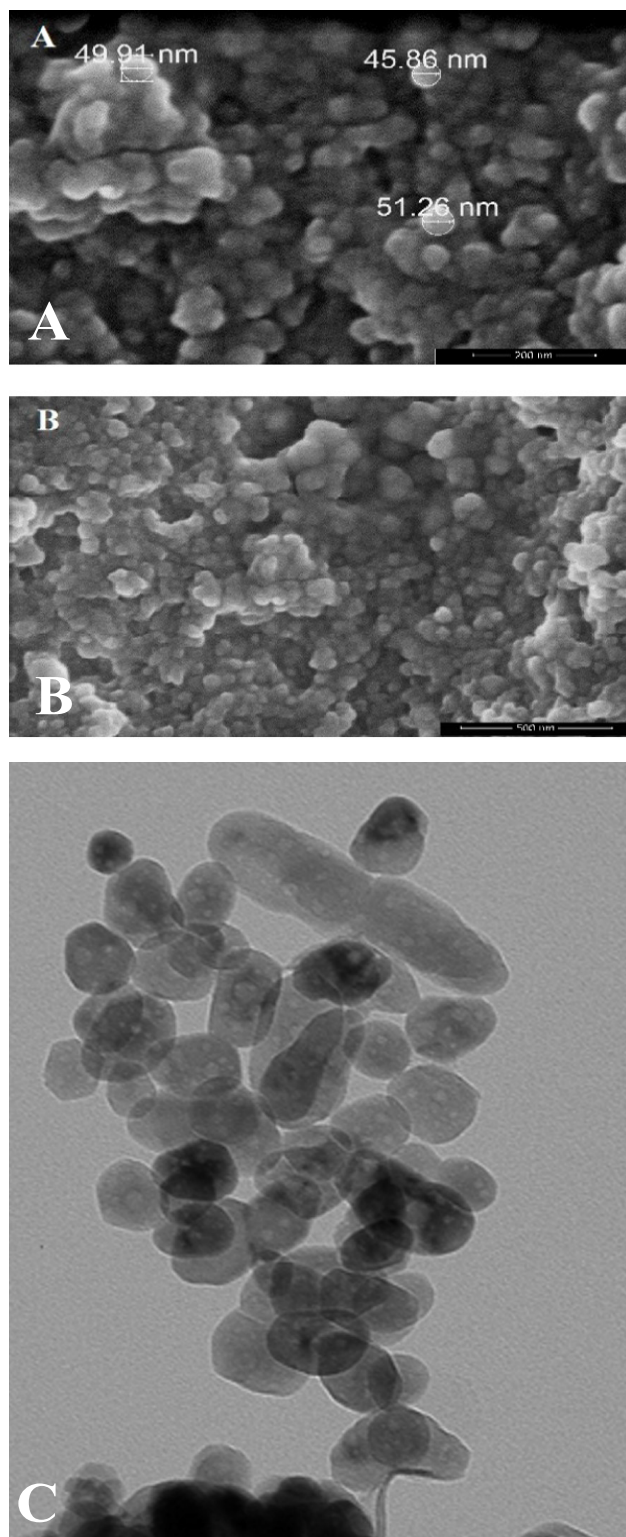


Fig. 1. SEM (A, B) and TEM (C) analysis of prepared iron oxide nanoparticles. A, scale bar: 200nm; B, scale bar: 500nm; C, magnification of 80,000X.

Figure 2B indicates FTIR patterns of bare iron oxide nano particles and epirubicin loaded iron oxide nanoparticles. FTIR pattern of epirubicin loaded particles showed both characteristic peaks of epirubicin and iron oxide nanoparticles confirming that epirubicin had adsorbed on the surface of the particles.

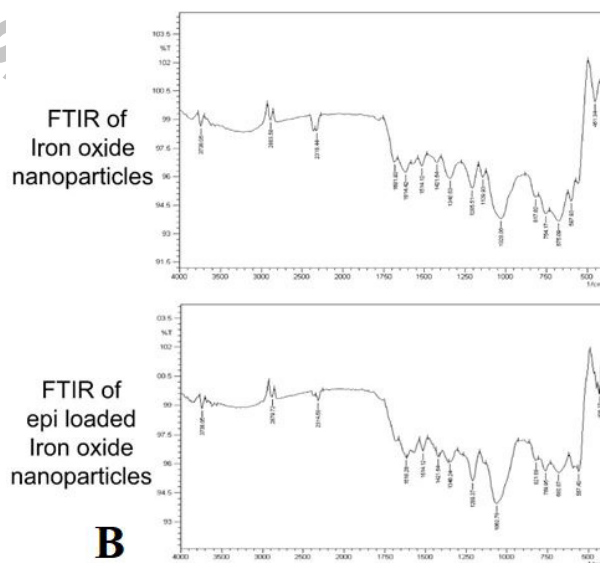
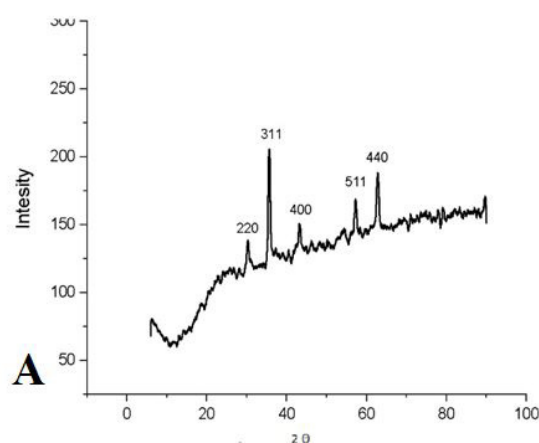


Fig. 2. XRD (A) analysis (B) and FTIR spectra of iron oxide nanoparticles, and drug loaded nanoparticles.

Epirubicin drug loading studies

Figure 3 shows the decrease in epirubicin concentration in the supernatant, over time; as a result of drug uptake by nanoparticles. Epirubicin was loaded on prepared iron oxide particles. Epirubicin showed maximum absorption at 498nm due to its conjugated structure. 1ml sample was removed from the mixture at specific time intervals and was centrifuged at 5000 g for 5 min. Supernatant was

collected for taking its absorbance at 498nm. The pellet was added back to the solution for further drug uptake.

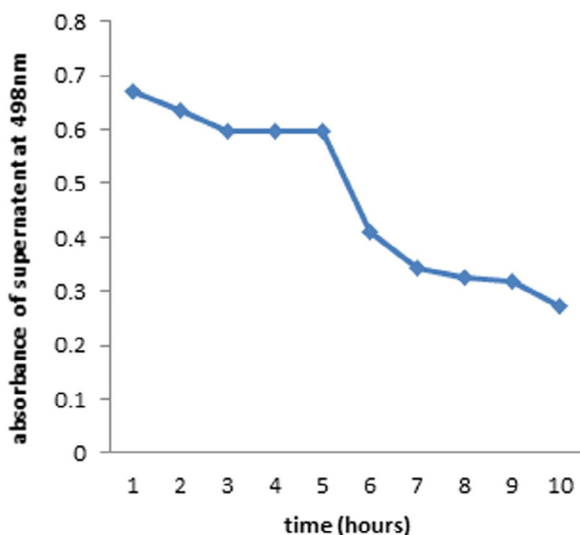


Fig. 3. Drug uptake by the particles resulted in reduction of absorbance of drug in the supernatant at 498nm. Particles were suspended in distilled water in an orbital shaker at 37 °C. 1 ml was removed from the suspension, centrifuged and absorbance of supernatant was taken at 498nm. The mixture was added back to the suspension for further uptake.

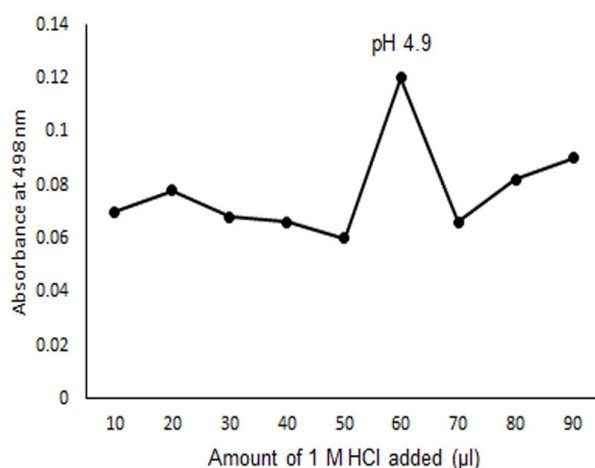


Fig. 4. The absorbance of epirubicin in the supernatant at 498nm versus the added amount of 1M HCl in μL (added to 4ml of epirubicin loaded iron oxide nanoparticle suspension in distilled water).

pH sensitive drug release

It can be clearly seen in Figure 4 that abrupt release

of the drug was observed at around pH 4.9 that is quite similar to the pH of the tumor microenvironment. Around the physiological pH a small amount of drug was released. However, addition of 60 μL of HCl to a 4 ml suspension of drug loaded iron oxide nanoparticles resulted in abrupt release of epirubicin and the pH of that suspension turned out to be 4.9. H⁺ acts as a molecular switch in detachment of drug from the nanoparticle. This is a clear indication that epirubicin drug loaded on iron oxide nanoparticles will make an abrupt release inside the tumor microenvironment.

Antimicrobial activity of naked and epirubicin loaded iron oxide nanoparticles

Figure 5 indicates the antimicrobial activity of NPs, assessed by measuring ZOI around the well with 50μg/100 μL concentration of naked iron oxide nanoparticles and Epirubicin loaded nanoparticles. The results revealed that Fe₂O₃ NPs showed 5mm zone of inhibition (ZOI) against *E. coli* and 4mm zone of inhibition against *S. aureus*. On other hand Epirubicin loaded nanoparticles were effective against *E. coli* and *S. aureus* resulting in 7mm and 6mm ZOI respectively. The increased zones of inhibition indicated that epirubicin loaded iron oxide nanoparticles showed enhanced antimicrobial activity as compared to naked nanoparticles.

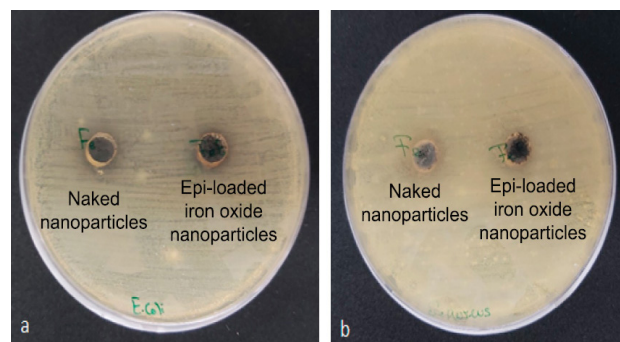


Fig. 5. Inhibitory effect of (a) Fe NPs and Epi loaded NPs on *E. coli* (Gram-negative bacteria) (b) Fe NPs and Epi loaded NPs on *S. aureus* (Gram positive bacteria) using well diffusion assay. Plates were placed in an incubator for 24 h before measuring the Zones of inhibition by both naked nanoparticles and epirubicin loaded particles.

Fluorescent microscopic analysis of epirubicin loaded iron oxide nanoparticles

In order to confirm that epirubicin was loaded on iron oxide nanoparticles, both the particles and drug loaded iron oxide nanoparticles were observed under the Olympus-BX 51 fluorescence microscope at 40X. In Figure 6 it can be seen that simple nanoparticles (smeared

on microscope slides) showed a plain blank image showing no fluorescence under the red channel while Epirubicin loaded on the nanoparticles showed bright red spots, confirming that the drug had been loaded on the surface of iron oxide nanoparticles. Images were assembled using Adobe Photoshop.

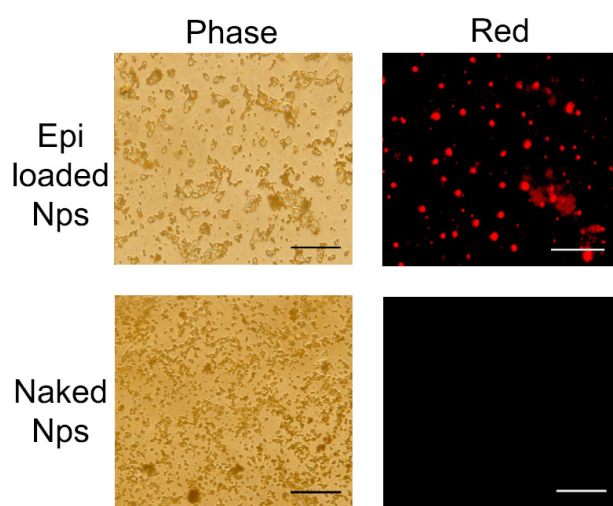


Fig. 6. Fluorescent microscopic images of nanoparticles; scale bar 125 μm ; nanoparticles (both naked and epirubicin loaded) suspended in distilled water were placed on a slide and were allowed to dry before imaging under the Olympus-BX 51 fluorescence microscope, 40X resolution.

In vitro cytotoxicity against human cancer cell line MDA-MB-231

Figure 7 shows that nanoparticle loaded drug had a potent cytotoxic effect on both MDA-MB-231/wild type and MDA-MB-231 epi-R cells. However, the survival rate varied. In both cell lines, epi-loaded iron oxide nanoparticles were able to show higher growth inhibition resulting in reduced viability with increasing drug dose.

It can be clearly seen in Figure 7 that at 20 μM epirubicin concentration cell viability of MDA-MB-231/wt cells turned out to be 65.725% which reduced to 54.7792% when the cells were exposed to 20 μM epirubicin loaded on iron oxide nanoparticles. On the other hand, at 20 μM epirubicin concentration, cell viability of MDA-MB-231/epi-R turned out to be 71.5924% which reduced to 58.193% when the cells were exposed to 20 μM epirubicin loaded on iron oxide nanoparticles

As indicated in Figure 7, naked nanoparticles had not affected the survival rate of both MDA-MB-231/wt and MDA-MB-231/epi-R cells, however at maximum concentration slight effect was observed. Percentage viability of MDA-MB-231/wt cells at highest concentration

of nanoparticles 82.058%, while it was 90.734% for MDA-MB-231/epi-R cells. At lower concentrations, nanoparticles did not affect the cells. MDA-MB-231/wt cells showed percentage viability of 54.7%, 20 μM epirubicin loaded on iron oxide nanoparticles while MDA-MB-231/epi-R showed viability of 59.193% at the same concentration. This difference confirms the resistant nature MDA-MB-231/epi-R cell line which had a slightly higher survival rate as compared to the wild type cells even in the presence of drug loaded nanoparticles.

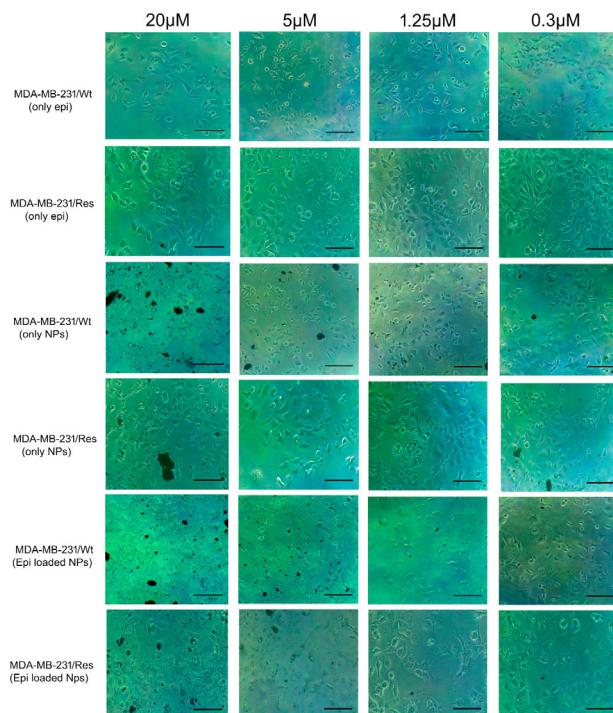
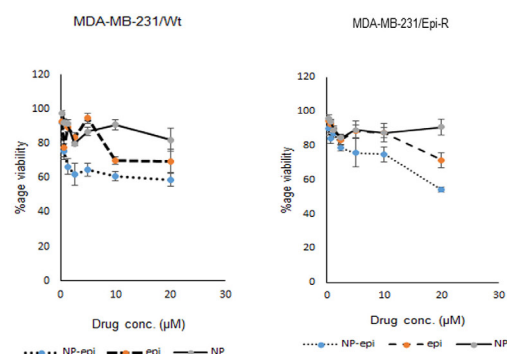


Fig. 7. Cell viability of breast cancer cell lines MDA-MB-231/epi R and MDA-MB-231/wt after incubation with epirubicin and epirubicin loaded iron oxide nanoparticles for 72 h, scale bar is 500 μm .

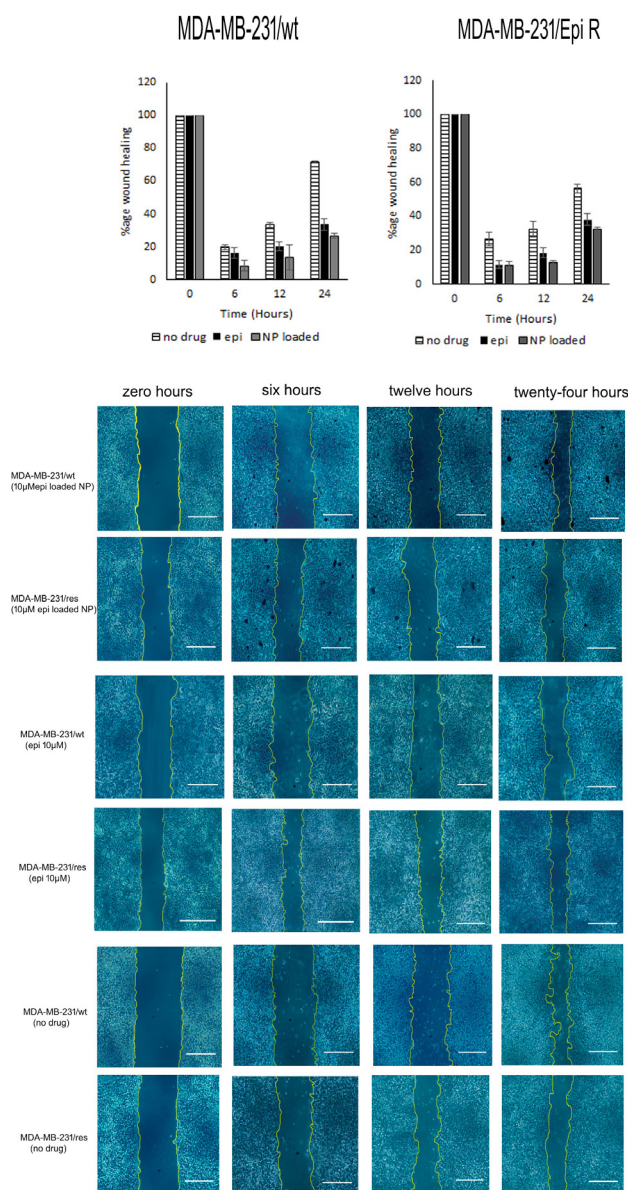


Fig. 8. Migration/wound healing assay of MDA-MB-231/wt and MDA-MB-231/Epi resistant cell line. Representative images of wound healing in both cell lines following exposure to 10 μ M epirubicin alone and epirubicin loaded on iron oxide nanoparticles at zero, six, twelve and twenty-four h. Scale bar 500 μ m.

Migration assay

The ability of drug loaded nanoparticles to bring changes to cancer metastasis was checked using both, MDA-MB-231/wt and epi-R cell lines through migration assay. Figure 8 shows delayed healing in case of drug loaded particles, when images were taken after 6, 12 and 24 h using an inverted phase contrast microscope.

MDA-MB-231/wt cells when incubated with 10 μ M epirubicin showed wound healing of 33.63%. The healing process was reduced remarkably to 26.8% when the cells were incubated with 10 μ M epirubicin, loaded on iron oxide nanoparticles. On the other hand, MDA-MB-231/epi-R cells also showed healing of 38.1% in case of incubation with 10 μ M epirubicin alone. Healing percentage reduced to 32.35% in case of incubation with 10 μ M epirubicin loaded on iron oxide nanoparticles.

DISCUSSION

Nanoparticles can be synthesized using various methods including natural resources like plants (Singh *et al.*, 2016). Green tea was used for the synthesis of iron oxide nanoparticles. The method was quick, cheap and easy to carry out. Particles were washed with water and ethanol to ensure the removal of all sorts of impurities. Particles were characterized using FTIR to ensure that the drug was loaded on the particle surface. XRD analysis was carried out to ensure that there were no impurities present in the particles.

Electron microscopy has shown that iron oxide nanoparticles possess the ability to bind to the cell wall of *E. coli*. They can even penetrate the membrane, cause vacuole formation and ultimately disrupt the cell wall (Armijo *et al.*, 2020). The prepared iron oxide nanoparticles in this research showed potent anti-microbial activity against *E. coli* (gram negative bacteria). The ZOI for iron oxide nanoparticles was 5mm while it increased by further 2 mm in case of epirubicin loaded particles resulting in 7mm (ZOI).

Epirubicin and doxorubicin have fluorescent properties whereby they show red fluorescence under the microscope (Duray *et al.*, 1998). In order to confirm the loading, particles were observed under fluorescent microscope. Drug loaded particles showed red fluorescence indicating the presence of loaded drug, whereas naked particles did not show any fluorescence.

In this study it was clearly observed that epirubicin loaded iron oxide nanoparticles showed higher cytotoxicity as compared to the drug alone. Also, delayed wound healing was observed in scratch assay indicating the potent effect of epirubicin loaded iron oxide nanoparticles.

CONCLUSION

Our findings reveal the importance of epirubicin loaded iron oxide nanoparticles in the treatment of breast cancer. Loading the drug reduces its potent effect on healthy cells ensuring targeted delivery to the target site.

Funding

The study received no external funding.

Ethical statement and IRB approval

Not applicable

Statement of conflict of interest

The authors have declared no conflict of interest.

REFERENCES

- Afzal, M., Safer, A.M. and Menon, M., 2015. Green tea polyphenols and their potential role in health and disease. *Inflammopharmacology*, **23**: 151–161. <https://doi.org/10.1007/s10787-015-0236-1>
- Ali, A., Zafar, H., Zia, Mul Haq., I, Phull, A.R., Ali, J.S. and Hussain, A., 2016. Synthesis, characterization, applications, and challenges of iron oxide nanoparticles. *Nanotechnol. Sci. Appl.*, **9**: 49-67. <https://doi.org/10.2147/NSA.S99986>
- Ameen, F., Srinivasan, P., Selvankumar, T., Kamala-Kannan, S., Nadhari, S.A., Almansob, A., Dawoud, T. and Govarthanan, M., 2019. Phytosynthesis of silver nanoparticles using *Mangifera indica* flower extract as bioreductant and their broad-spectrum antibacterial activity. *Bioorg. Chem.*, **88**: 102970. <https://doi.org/10.1016/j.bioorg.2019.102970>
- Arami, H., Khandhar, A., Liggitt, D. and Krishnan, K.M., 2015. *In vivo* delivery, pharmacokinetics, biodistribution and toxicity of iron oxide nanoparticles. *Chem. Soc. Rev.*, **44**: 8576–8607. <https://doi.org/10.1039/C5CS00541H>
- Armijo, L.M., Wawrzyniec, S.J., Kopciuch, M., Brandt, Y.I., Rivera, A.C., Withers, N.J., Cook, N.C., Huber, D.L., Monson, T.C., Smyth, H.D.C. and Osiński, M., 2020. Antibacterial activity of iron oxide, iron nitride, and tobramycin conjugated nanoparticles against *Pseudomonas aeruginosa* biofilms. *J. Nanobiotechnol.*, **2020**: 18. <https://doi.org/10.1186/s12951-020-0588-6>
- Awwad, A.M. and Salem, N.M., 2012. A green and facile approach for synthesis of magnetite nanoparticles. *Nanosci. Nanotechnol.*, **2**: 208–213. <https://doi.org/10.5923/j.nn.20120206.09>
- Cheng, R., Meng, F., Deng, C., Klok, H.A. and Zhong, Z., 2013. Dual and multi-stimuli responsive polymeric nanoparticles for programmed site-specific drug delivery. *Biomaterials*, **34**: 3647–3657. <https://doi.org/10.1016/j.biomaterials.2013.01.084>
- Duncan, R., 2003. The dawning era of polymer therapeutics. *Nat. Rev. Drug Dis.*, **2**: 347–360. <https://doi.org/10.1038/nrd1088>
- Duray, P.H., Cuono, C.B. and Madri, J.A., 1986. Demonstration of cutaneous doxorubicin extravasation by rhodamine-filtered fluorescence microscopy. *J. Surg. Oncol.*, **31**: 21–25. <https://doi.org/10.1002/jso.2930310104>
- Farokhzad, O.C. and Langer, R., 2009. Impact of nanotechnology on drug delivery. *ACS Nano.*, **3**: 16–20. <https://doi.org/10.1021/nn900002m>
- Jagwani, D. and Hari, K.P., 2021. Nature's nano-assets: Green synthesis, characterization techniques and applications. A graphical review. *Mater. Today Proc.*, **46**: 2307–2317. <https://doi.org/10.1016/j.matpr.2021.04.185>
- Liang, X.J., Chen, C., Zhao, Y. and Wang, P.C., 2010. Circumventing tumor resistance to chemotherapy by nanotechnology. *Meih. Mol. Biol.*, **596**: 467-488. https://doi.org/10.1007/978-1-60761-416-6_21
- Muthu, M.S., Rajesh, C.V., Mishra, A. and Singh, S., 2009. Stimulus-responsive targeted nanomicelles for effective cancer therapy. *Nanomedicine*, **4**: 657–667. <https://doi.org/10.2217/nmm.09.44>
- Oskam, G., 2006. Metal oxide nanoparticles: Synthesis, characterization and application. *J. Sol-gel Sci. Technol.*, **37**: 161–164. <https://doi.org/10.1007/s10971-005-6621-2>
- Regu, J.T., Suchithra, P.S. and Yong, Y.J., 2020. Tumor microenvironment-stimuli responsive nanoparticles for anticancer. *Front. Mol. Biosci.*, **7**: 610533. <https://doi.org/10.3389/fmolb.2020.610533>
- Ruenraroengsak, P., Cook, J.M. and Florence, A.T., 2010. Nano system drug targeting: Facing up to complex realities. *J. Contr. Release.*, **141**: 265–276. <https://doi.org/10.1016/j.jconrel.2009.10.032>
- Saeed, M., Ren, W. and Wu, A., 2018. Therapeutic applications of iron oxide based nanoparticles in cancer: basic concepts and recent advances. *Biomater. Sci.*, **6**: 708–725. <https://doi.org/10.1039/C7BM00999B>
- Saif, S., Tahir, A. and Chen, Y., 2016. Green Synthesis of Iron Nanoparticles and Their Environmental Applications and Implications. *Nanomaterials*, **6**: 209. <https://doi.org/10.3390/nano6110209>
- Sindhvani, S., Syed, A.M., Ngai, J., Kingston, B.R., Maiorino, L., Sothschild, J., MacMillan, P., Zhang, Y., Rajesh, N.U., Hoang, T., Wu, J.L.Y., Wilhelm, S., Zilman, A., Gadde, S., Sulaiman, A., Ouyan, B., Lin, Z., Wang, L., Egeblad, M. and Chan, W.C.W., 2020. The entry of nanoparticles into solid tumours. *Nat. Mater.*, **19**: 566-575. <https://doi.org/10.1038/s41563-019-0566-2>
- Singh, P., Kim, Y.J., Zhang, D. and Yang, D.C., 2016. Biological synthesis of nanoparticles from plants

- and microorganisms. *Trends Biotech.*, **34**: 588-599. <https://doi.org/10.1016/j.tibtech.2016.02.006>
- Unsoy, G., Khodadust, R., Yalcin, S., Mutlu, P. and Gunduz, U., 2014. Synthesis of Doxorubicin loaded magnetic chitosan nanoparticles for pH responsive targeted drug delivery. *Eur. J. Pharm. Sci.*, **62**: 243–250. <https://doi.org/10.1016/j.ejps.2014.05.021>
- Weng, X., Guo, M., Luo, F. and Chen, Z., 2017. One-step green synthesis of bimetallic Fe/Ni nanoparticles by eucalyptus leaf extract: Biomolecules identification, characterization and catalytic activity. *Chem. Eng. J.*, **308**: 904–911. <https://doi.org/10.1016/j.cej.2016.09.134>
- Yew, Y.P., Shameli, K., Miyake, M., Ahmad, Khairudin, N.A.A., Mohamad, S.E. and Naiki, T., 2020. Green biosynthesis of superparamagnetic magnetite Fe₃O₄ nanoparticles and biomedical applications in targeted anticancer drug delivery system: A review. *Arab. J. Chem.*, **13**: 2287-2308. <https://doi.org/10.1016/j.arabjc.2018.04.013>
- Yue-feng, R., Wei, C., Xing-Guang, L., Yong-Zhuo, H., Jing, M., Lin, L., Yan, L., Xing-Guo, Z, Ben, W., Rui-Kang, T., Zhong, C. and Xiao-Yang, L., 2008. Epirubicin-loaded superparamagnetic iron-oxide nanoparticles for transdermal delivery: Cancer therapy by circumventing the skin barrier. *Drug Deliv.*, **2**: 477–484.
- Zylberberg, C. and Matosevic, S., 2016. Pharmaceutical liposomal drug delivery: A review of new delivery systems and a look at the regulatory landscape. *Drug Deliv.*, **23**: 3319–3329. <https://doi.org/10.1080/10717544.2016.1177136>

Online First Article